



## Protective effects of recombinant lactoferrin with different iron saturations on enteritis injury in young mice

L. L. Fan,\* Q. Q. Yao,\* H. M. Wu,<sup>ORCID</sup> F. Wen, J. Q. Wang,<sup>ORCID</sup> H. Y. Li,<sup>†</sup> and N. Zheng<sup>†</sup><sup>ORCID</sup>

Key Laboratory of Quality & Safety Control for Milk and Dairy Products of Ministry of Agriculture and Rural Affairs, Institute of Animal Science, Chinese Academy of Agricultural Sciences, Beijing 100193, P. R. China

### ABSTRACT

Infant intestinal development is immature and, thus, is vulnerable to bacterial and viral infections, which damage intestinal development and even induce acute enteritis. Numerous studies have investigated that lactoferrin (LF) has protective effects on the intestine and may play a role in preventing intestinal inflammation in infants. Lactoferrin is divided into 2 types, namely apo-LF and holo-LF, depending on the degree of iron saturation, which may affect its bioactivities. However, the role of LF iron saturation in protecting infant intestinal inflammation has not been clearly clarified. Therefore, in this study, young mice models with intestinal damage induced by lipopolysaccharides (LPS) *in vivo* and primary intestinal epithelial cells *in vitro* were constructed to enteritis injury in infants for investigation. The apo-LF and holo-LF were subsequently applied to the mouse models to investigate and compare their levels of protection in the intestinal inflammatory injury, as well as to identify which LF was most active. Moreover, the specific mechanism of the LF with optimal iron saturation was further investigated through Western blot assay. Results demonstrated that disease activity index, shortened length of colon tissue, and histopathological score were significantly decreased in the apo-LF group compared with those of the LPS group and the holo-LF group. In the apo-LF group, the concentration of LPS in the intestinal tract and the number of gram-negative bacteria colonies decreased significantly and the expression levels of proinflammatory factors in the colon tissue were downregulated, in comparison with those in the LPS group. The findings of this study thus verify that apo-LF can significantly alleviate enteritis injury caused by LPS, through regulating the PPAR- $\gamma$ /PPKFB3/NF- $\kappa$ B inflammatory pathway.

**Key words:** lactoferrin, lipopolysaccharides, iron saturation, enteritis

### INTRODUCTION

The intestine is one of the largest organs in the body, with 60% to 70% of immune cells and a highly complex immune barrier system (Grisham and Yamada, 1992; Richter et al., 1997; Scaldaferrri and Fiocchi, 2007). Intestinal epithelial cells can not only respond to external stimuli themselves by stimulating the expression of inflammatory factors and chemokines through corresponding signaling pathways, but they can also recruit more white blood cells to kill and remove damaged cells or foreign pathogens (Peterson and Artis, 2014). Since intestinal development in infants is immature, their immunity is weak, making them vulnerable to bacterial and viral infections, which can cause impaired intestinal development and even induce acute enteritis (Battersby et al., 2017, 2018). Indeed, acute enteritis is a global public health problem and the second highest cause of morbidity and death in children under 5 yr of age, causing more than 1 million deaths annually and accounting for approximately 15% of all infant and young child deaths (Black et al., 2010). The North American Society for Pediatric Gastroenterology and Hepatology and Nutrition estimates that the overall annual incidence of enteritis in children under 3 yr of age is 1.3 per person in developed countries and 3 per person in developing countries (Fitzsimons, 2013). Studies have found that acute enteritis can damage intestinal villous epithelial cells, leading to the malabsorption of nutrients, which seriously affects the growth and development of infants (Villaseca et al., 2005; Nabulsi et al., 2015). Furthermore, the disease not only causes serious emotional distress and fatigue for parents and children, but also increases the risk of complications due to malnutrition or impaired immune function in children (Nabulsi et al., 2015). Therefore, intestinal development is crucial to the health of infants and young children and the improvement of intestinal immunity in infants has long been of scientific concern in the fields of nutrition, food, and medicine (Zhou et al., 2015; Yu et al., 2016).

Received October 13, 2021.

Accepted February 16, 2022.

\*These authors contributed equally to this work.

<sup>†</sup>Corresponding authors: [thufit2012@126.com](mailto:thufit2012@126.com) and [zhengnan\\_1980@126.com](mailto:zhengnan_1980@126.com)

A nonheme iron binding glycoprotein and a member of the transferrin family, with a molecular weight of 80 kDa, lactoferrin (**LF**) is mainly expressed and secreted by mammary epithelial cells. Lactoferrin exhibits a variety of biological activities, including participating in iron metabolism, antiinflammatory, antibacterial, antiviral, anticancer, and antioxidant functions, and the regulation of immunity (Hering et al., 2017; Li et al., 2019; Niaz et al., 2019) and is, therefore, considered a milk protein with great research and development prospects. Due to its ability to stably and reversibly bind 2 ferric ions ( $\text{Fe}^{3+}$ ; Baker and Baker, 2004), LF is considered to have 2 different iron binding states: iron-deficient lactoferrin (**apo-LF**) and iron-saturated lactoferrin (**holo-LF**). Studies have shown that the conformation of LF changes greatly as it binds and releases iron. Compared with apo-LF, holo-LF has a more stable and compact structure (Grossmann et al., 1992). Furthermore, LF's level of iron saturation has been found to affect its physiological functioning. Lu et al. (2008) showed that with the increase of iron saturation, the bacteriostatic ability of LF decreased. Through the construction of breast tumor models, it was also found that iron saturation had an effect on the tumor inhibition activity of LF, in which apo-LF is strongest (Kanwar et al., 2015). Jiang and Lönnerdal showed that apo-LF stimulated crypt cell proliferation significantly more than holo-LF in an in vitro test. However, holo-LF maintains high stability, especially when heated and stored for a long time, and it does not easily form polymers or degrade. For these reasons, holo-type LF is often added to milk products such as infant's powder (Jiang and Lönnerdal, 2012).

Based on the above introductory data, animal and cell models of an LPS-induced intestinal inflammation in infants were simulated and constructed in this study to verify the protective effects of LF with different iron saturations via the regulation of the PPAR- $\gamma$ /PPKFB3/NF- $\kappa$ B signaling pathway and also to analyze their interaction mechanisms.

## MATERIALS AND METHODS

### Chemicals

Human recombinant lactoferrin (holo-LF) expressed in rice was purchased from Sigma (L1294-1G, the purity  $\geq 90\%$ ). Using holo-LF as raw material, apo-LF was prepared according to the patent "a method for preparing lactoferrin with required iron saturation" (Luo et al., 2020). By adding citrate buffer (0.5 M) with a pH of 2 to the holo-LF solution (0.1 M), the molar volume ratio of citrate buffer to holo-LF was 3:1, then adjusting the pH value of the solution to 5;

next, the LF solution could be made into a sample with an iron saturation of 4.1%, which was regarded as the apo-type LF in the present study (Luo et al., 2020). Lipopolysaccharide (L8880-10 mg, purity  $\geq 99\%$ ) and inflammatory cytokine kits (mouse IL-1 $\beta$  ELISA kit, mouse IL-6 ELISA kit, mouse TNF- $\alpha$  ELISA kit, and mouse IFN $\gamma$  ELISA kit) were purchased from Beijing Solarbio Technology Co. Ltd., and a cell counting kit-8 (CCK-8) was purchased from Solarbio. Hematoxylin-eosin (**HE**) and 3,3'-diaminobenzidine (**DAB**) staining kits were from Wuhan Seville Biotechnology Co. Ltd.

### Animal Experiments

Forty-eight 2-wk-old male C57BL/6J mice weighing about 13 g were purchased from Beijing Weishenghe Experimental Animal Technology Co., Ltd. (Beijing, China; license no. scxk 2012-0001). The mice were randomly divided into 6 groups: apo-LF group, holo-LF group, LPS group, apo-LF+LPS group, holo-LF+LPS group, and control group, with 8 mice in each group ( $n = 8$ ).

During the 14-d experiment period, mice in both the apo-LF group and the holo-LF group were intragastrically administered daily with LF (100 mg/kg BW). Mice in the LPS treatment group were intraperitoneally injected with LPS (10 mg/kg BW) daily on d 10 to 14. Mice in the apo-LF+LPS treatment group and holo-LF+LPS treatment group were gavaged with LF (100 mg/kg BW) every day for 1 to 14 d, and these mice were also intraperitoneally injected with LPS (10 mg/kg BW) every day on d 10 to 14. Mice in the control group were fed normally. On d 15, the mice were killed by cervical dislocation, and their colon and intestinal tissues were collected. The experiment design is shown in Figure 1A. Before the formal experiment, these mice were fed normally for 5 d. The protocols in this study are those approved by the Committee on the Ethics of Animal Experiments of the Chinese Academy of Agricultural Sciences (Beijing, China; permission number: IAS202104), conforming to internationally accepted principles for the care and use of experimental animals (NRC, 2001). Surgical procedures were performed under inhalational anesthesia with ether and all efforts were made to minimize the suffering of the mice.

### Disease Activity Index Calculation and Colon Length Measurement

Body weight, fecal traits, and recessive or dominant fecal bleeding were recorded daily. Disease activity indices (**DAI**) of the mice in each group were calculated according to the classical method (Murano et al., 2001), and scoring criteria are presented in Table 1.

The colitis DAI was calculated as (weight loss + stool traits + bleeding)/3. Colon lengths were measured using a Vernier caliper.

**Detection of LPS Concentration in Intestinal Contents**

Following euthanasia, we mainly took the tissue (about 2 cm) away from the middle part of the colon.

The contents of the mouse colon were removed and we weighed 100 mg accurately, and normal saline was added into the colon tissue to prepare 10% homogenate and centrifuged (4°C, 1,000 × g, 10 min). Next, 0.5 mL of supernatant was measured, 0.5 mL of normal saline was added into the supernatant to dilute it, and the prepared samples and standards were used to detect LPS concentration according to the lipopolysaccharide ELISA kit. The values at 450 nm were read with a

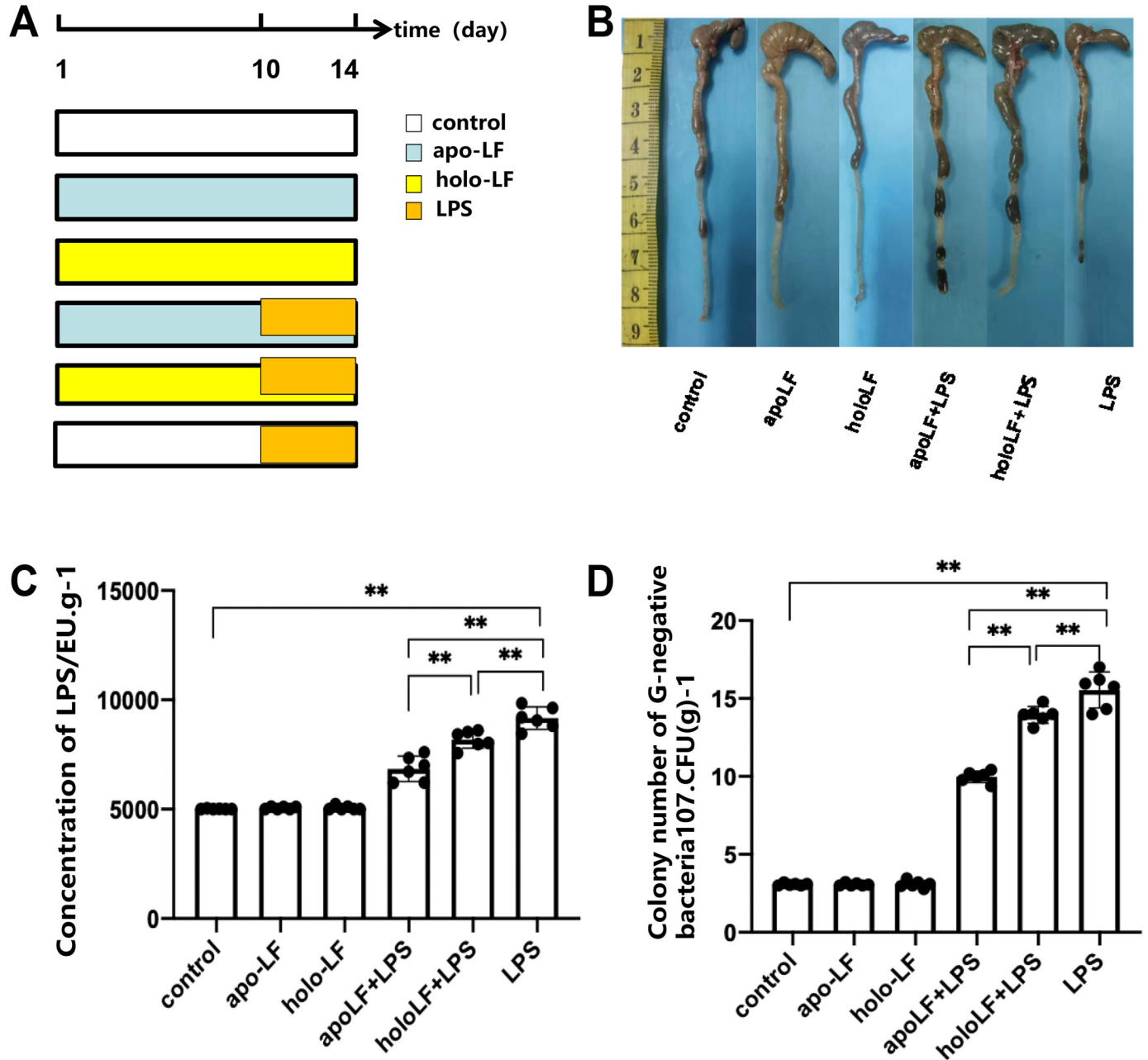


**Figure 1.** (A) Animal experiment design, (B) colons of young mice, (C) LPS concentrations in intestinal contents, and (D) changes in gram (G)-negative bacteria. EU = endotoxin units. The data are shown as mean ± SD. Differences between groups were analyzed using Student's *t*-test. \*\**P* < 0.01, compared with the control, n = 8. apo-LF = iron-deficient lactoferrin; holo-LF = iron-saturated lactoferrin.

**Table 1.** Disease activity indices<sup>1</sup>

Score	Weight loss (%)	Stool <sup>2</sup> consistency	Occult or gross bleeding
0	(–)	Normal	Normal
1	1–5		
2	5–10	Loose	Guaiaic (+)
3	11–15		
4	>15	Diarrhea	Gross bleeding

<sup>1</sup>Disease activity indices = sum of weight loss, stool consistency, and bleeding scores/3.

<sup>2</sup>Normal: well-formed pellets; loose: pasty stools that do not stick to the anus; diarrhea: liquid stools that stick to the anus.

Microplate Reader (Thermo Scientific). The result is finally expressed in endotoxin units per gram (Li et al., 2021a; Xia et al., 2021).

### Detection of Gram-Negative Bacteria Colonies

Following euthanasia, the contents of the mouse colon tissue were removed and 100 mg was weighed accurately; normal saline was added into the sample to prepare 10% homogenate, and then it was centrifuged (4°C, 1,000 × *g*, 10 min). The supernatant was poured into the plate with broth medium and cultured for 24 h in the anaerobic incubator (Plas-Lab 855-AC and 855-ACB; Plas Labs Inc.). Then, a small number of bacteria was picked up with an inoculation ring and evenly coated on clean slides. Bacteria were stained with ammonium oxalate crystal violet for 1 min, and normal saline was used to wash the floating color. The slides were soaked in potassium iodide solution for 1 min and then decolorized with ethanol (95%) for 30 s. The gram-negative bacteria colonies were observed and counted using a microscope (Zhao et al., 2015; Zhang et al., 2018).

### Detection of Serum Inflammatory Cytokines

The concentrations of IL-1 $\beta$ , IL-6, TNF- $\alpha$ , and INF- $\gamma$  factors in the mice colon tissue were measured via ELISA, according to the ELISA kit instructions. Briefly, 500  $\mu$ L of serum was mixed with a cocktail of biotinylated detection antibodies and incubated with a membrane spotted with capture antibodies. Unbound material was washed off and the bound cytokines were measured by the chemiluminescence method as instructed. The orifice plate was then placed in the multifunction enzyme label (Microplate Reader) instrument and the absorbance (optical density value) of each orifice was measured at the wavelength of 450 nm.

### HE and DAB Staining

For the HE stains, sections of the colonic tissues of the mice were fixed in 4% paraformaldehyde, then

dehydrated, embedded in paraffin, sectioned, stained, and sealed with neutral gum. The morphology of the colonic mucosa was observed under light microscope.

For DAB detection, sections of the colonic tissue of the young mice were fixed in 4% paraformaldehyde, then dehydrated, embedded in paraffin, sectioned, and stained. The DAB was then quickly added to observe the staining, whereafter the dye solution was poured out. The time for color development was controlled within 3 to 10 min.

### Isolation and Culture of Primary Intestinal Epithelial Cells

The intestines of young mice were excised under sterile conditions and the mesentery was removed, washed with PBS, and centrifuged at 1,500 × *g* for 5 min at 4°C; the course was repeated for about 3 times until the supernatant was transparent. The intestines were washed with a serum-free Dulbecco's Modified Eagle Medium (DMEM)/F12 medium containing double antibodies (penicillin-streptomycin solution, 100×) 3 times, and then cut into fragments of approximately 1 mm<sup>3</sup>. The mesenteric supernatant was then washed with a serum-free DMEM/F12 medium containing penicillin-streptomycin solution (100×) and centrifuged at 1,000 × *g* for 3 min at 4°C. Thereafter, an enzymatic digestion solution (300 U/mL collagenase XI, 0.1 mg/mL neutral protease) was added. The mixture was oscillated at 37°C for digestion for 30 min; then, fetal bovine serum was added to terminate the digestion and the mixture was centrifuged at 1,000 × *g* for 15 min at 4°C, whereafter the supernatant was discarded. Next, the cells were inoculated in a 10-cm-diameter cell dish and cultured at 37°C in a 5% CO<sub>2</sub> incubator. After the cells adhered to the dish wall, we observed the dish with an optical microscope, drew the small intestinal epithelial cell colonies with a marker pen, and scraped the fibroblast area with a glass scraper. The cells were washed with PBS and the supernatant was discarded, the epithelial cells were digested with trypsin-EDTA, and the suspension was collected into the centrifuge tube and centrifuged for 5 min at 1,000 × *g* at 4°C.

The precipitate was resuspended with fresh DMEM/F12 culture medium, which was transferred to a new culture dish for further culturing. The above steps were repeated 3 to 5 times until the microscopic field of vision was basically all epithelial cells.

### Cell Culture and Cell Viability Assay

The primary intestinal epithelial cells were cultured in DMEM/F12 medium (containing 10% PBS, 500  $\mu$ L of penicillin and streptomycin) in an incubator (37°C, 5% CO<sub>2</sub>). Cells were planted into 96-well plates and cultured for at least 24 h. Thereafter, cells were first exposed to apo-LF (10 g/L) for 4 h, and LPS (1 mg/L) was added and they were cocultured together for another 48 h. A cell counting kit-8 (CCK-8) was used to detect cell viability, and the appropriate dose of LF was further selected to detect the cell viability with the combination of apo-LF+LPS, to further verify the protective effect of LF.

### Quantitative PCR and Western Blotting Used to Select the Appropriate LF Agent for Cells

In the cell model test, we seeded the mouse intestinal epithelial cells, and the cell density reached about 80%. The cells were divided into 8 groups ( $n = 3$ /group), control group (without any drugs), LF (1 g/L) group, LF (5 g/L) group, LF (10 g/L) group, LPS group, LPS+LF (1 g/L) group, LPS+LF (5 g/L) group, and LPS+LF (10 g/L) group. The cells were cultured for 48 h, and the cells were collected for western blotting (WB) and quantitative PCR (q-PCR) tests. The q-PCR method was as follows: we extracted the RNA of cells by the Trizol method, added 0.2 mL of chloroform, and mixed vigorously for 15 s at 4°C, 12,000  $\times g$ , for 10 min. We carefully took the upper water sample layer (the volume is about 60% of the added Trizol) and transferred it to a new Eppendorf tube. We did not absorb the protein. We added 0.5 mL of isopropanol, mixed it upside down, and placed it at 25°C for 10 min and at 4°C, 12,000  $\times g$ , for 10 min (or until colloidal flake precipitation could be seen at the bottom of the tube), and removed the supernatant. Then, 1 mL of 75% ethanol precipitated RNA (the same amount as Trizol), and we shook and mixed the sample. At 4°C, 10,000  $\times g$ , 10 min, the supernatant was absorbed as thoroughly as possible, but loss of RNA precipitation was prevented, and it was allowed to stand to volatilize the ethanol. Finally, 50  $\mu$ L of DEPC water was added to dissolve RNA. We used the  $2^{-\Delta\Delta C_t}$  method to quantify the relevant expression of the target gene and normalized it to the expression of  $\beta$ -actin. To detect the inflammatory signaling pathways in the primary intestinal epithelial cells, western

blotting assays were performed. After 48 h of LF (1, 5, and 10 g/L) treatment, 4 types of cells were collected, namely the apo-LF cells, LPS cells, apo-LF+LPS cells, and the control. Total protein in the cell samples was extracted using a protein extraction kit (Beijing Solarbio Science) and determined via a BCA protein assay kit (Beijing Solarbio Science). After heat treatment at 95°C for 10 min, protein samples were added to 10% SDS-polyacrylamide gel and electrophoresis was performed. Proteins were then transferred to the nitrocellulose membrane via trans-blot (Tanon) and the filter was sealed in a Tris-buffered saline with Tween solution with 2% BSA at room temperature for 1.5 h. Thereafter, primary antibodies PPAR- $\gamma$ , PFKFB3, NF- $\kappa$ B, IL-6, TNF- $\alpha$ , and internal reference  $\beta$ -actin were added to the proteins and they were incubated at room temperature for 120 min. The membrane was washed with phosphate buffered solution with Tween 20, the secondary antibody was added, and the membrane was co-incubated at room temperature for 60 min. Finally, the membrane was detected with enhanced chemiluminescence reagent and image analysis software (Image J1.53a; National Institutes of Health) was used for color exposure.

### Data Analysis

All data are expressed as means and standard deviations. Data analysis was performed using GraphPad Prism 6.0 software (GraphPad). Student's *t*-test and one-way ANOVA were used for statistical analyses, and  $P < 0.05$  was considered to indicate a significant difference between the groups.

## RESULTS

### DAI of Young Mice With Enteritis

As the results shown in Table 2 demonstrate, the mice in the control group, the separate apo-LF group, and the holo-LF group exhibited normal activities, weight gain, and stools, and their DAI were found to be stable and to have low levels. However, it is obvious that the DAI of young mice in the apo-LF group was better than that in the holo-LF group.

### Colon Length Comparison Among Different Groups

The average colon length of mice in the normal, apo-LF, and holo-LF groups was approximately 8.5 cm, whereas that of the LPS group had shortened to 6.0 cm, which was significantly shorter than that of the control group ( $P < 0.05$ ; Figure 1B). Compared with the control group, the average colon length of the mice in the

apo-LF+LPS and holo-LF+LPS groups had shortened by 1.0 cm ( $P < 0.05$ ), but this was still significantly ( $P < 0.05$ ) longer than that of the LPS group (Figure 1B). These results, thus, indicate that apo-LF and holo-LF significantly reduced colon shortening in the mice with LPS-induced enteritis.

### LPS Concentration in Intestinal Contents

As shown in Figure 1C, the LPS concentration in the intestines of the LPS group was found to be significantly higher than that in the control group. Moreover, compared with that of the LPS group, the LPS in the intestinal contents of the apo-LF+LPS group had significantly decreased. These results indicate that apo-LF significantly downregulated the LPS concentration in intestinal contents; however, the improvement of intestinal LPS concentration in holo-LF group was not significant (Figure 1C).

### Analysis of Gram-Negative Bacteria Colonies in Mice Feces

The number of gram-negative bacteria colonies in the intestinal tracts of the mice in the LPS group had increased significantly, whereas the number of gram-negative bacteria in the apo-LF+LPS group were significantly lower, indicating that apo-LF inhibited the growth of gram-negative bacteria (Figure 1D). The number of gram-negative bacteria in the holo-LF+LPS group was not significantly different from that of the LPS group; however, it was significantly higher than that of the apo-LF+LPS group, and it can be seen from the figure that the effect of apo-LF was better than that in the holo-LF group (Figure 1D).

### Expression of Inflammatory Factors in Colonic Tissue of Young Mice

As shown in Figure 2, the expression levels of TNF- $\alpha$ , IL-1 $\beta$ , and IL-6 in the LPS group were significantly higher than those of the control group ( $P < 0.05$ ). The levels of these inflammatory factors in the apo-LF+LPS group were significantly lower than those in the LPS

group, and there were no obvious differences between the levels of these factors in the holo-LF+LPS and LPS groups ( $P > 0.05$ ; Figure 2A–C). The inhibitory effect of apo-LF on the expression of proinflammatory factors was, thus, significantly stronger than that in the holo-LF group. The expression level of antiinflammatory factor INF- $\gamma$  in the colon tissue of the LPS group was significantly lower than that of the normal group ( $P < 0.05$ ; Figure 2D), thus verifying that the inhibitory effect of apo-LF on the expression of antiinflammatory factors was significantly stronger than that of holo-LF.

### HE Stain of Colonic Tissue

The pathological staining results demonstrated that the structure of the colon tissue in the control group consisted of regular glands, and no inflammatory cell infiltration, edema, congestion, erosion, ulceration, or other conditions were observed (Figure 3A). In the LPS group, the colonic mucosal epithelium was found to be partially defective, the glands were reduced and disorderly, mucosal edema and congestion were obvious, a large number of inflammatory cells had been infiltrated, goblet cells were reduced, and ulcer lesions had formed (Figure 3A). Pathological results in both the apo-LF+LPS and holo-LF+LPS groups showed alleviated colonic tissue damage, reduced mucosal ulcers, regular glandular structures, and reduced congestion and edema, accompanied by a small amount of inflammatory cell infiltration. Furthermore, the protective effect of the apo-LF was significantly more obvious than in the holo-LF group (Figure 3A).

### DAB Staining Analysis of the Intestinal Tracts of Young Mice

As shown by the DAB staining results in Figure 3B, compared with the normal group, the LPS group showed a large area of brown positive reaction and obvious inflammation to inflammatory factors. The PPAR- $\gamma$ , PFKFB3, and NF- $\kappa$ B of the LPS group and normal group showed significant ( $P < 0.05$ ) differences in B levels, indicating that these factors were involved in LPS-induced colon tissue inflammation (Figure 3B).

**Table 2.** Disease activity indices (DAI) of mice with enteritis (mean  $\pm$  SD)<sup>1</sup>

Item	Control	Apo-LF	Holo-LF	LPS	Apo-LF+LPS	Holo-LF+LPS
DAI score	0 $\pm$ 0.19 <sup>a</sup>	0 $\pm$ 0.20 <sup>a</sup>	0.3 $\pm$ 0.08 <sup>a</sup>	9.5 $\pm$ 0.42 <sup>b</sup>	5.5 $\pm$ 0.33 <sup>c</sup>	8.9 $\pm$ 0.16 <sup>b</sup>
Colon length	8.0 $\pm$ 0.51 <sup>a</sup>	8.01 $\pm$ 0.49 <sup>a</sup>	8.0 $\pm$ 0.48 <sup>a</sup>	5.0 $\pm$ 0.69 <sup>b</sup>	6.5 $\pm$ 0.77 <sup>c</sup>	6.0 $\pm$ 0.96 <sup>b</sup>
Histopathological score	0.17 $\pm$ 0.01 <sup>a</sup>	0.15 $\pm$ 0.01 <sup>a</sup>	0.18 $\pm$ 0.02 <sup>a</sup>	3.71 $\pm$ 0.30 <sup>b</sup>	2.79 $\pm$ 0.42 <sup>c</sup>	3.58 $\pm$ 0.37 <sup>b</sup>

<sup>a–c</sup>Data within a row with different letters indicate significant differences ( $P < 0.05$ ).

<sup>1</sup>Apo-LF = iron-deficient lactoferrin; holo-LF = iron-saturated lactoferrin.

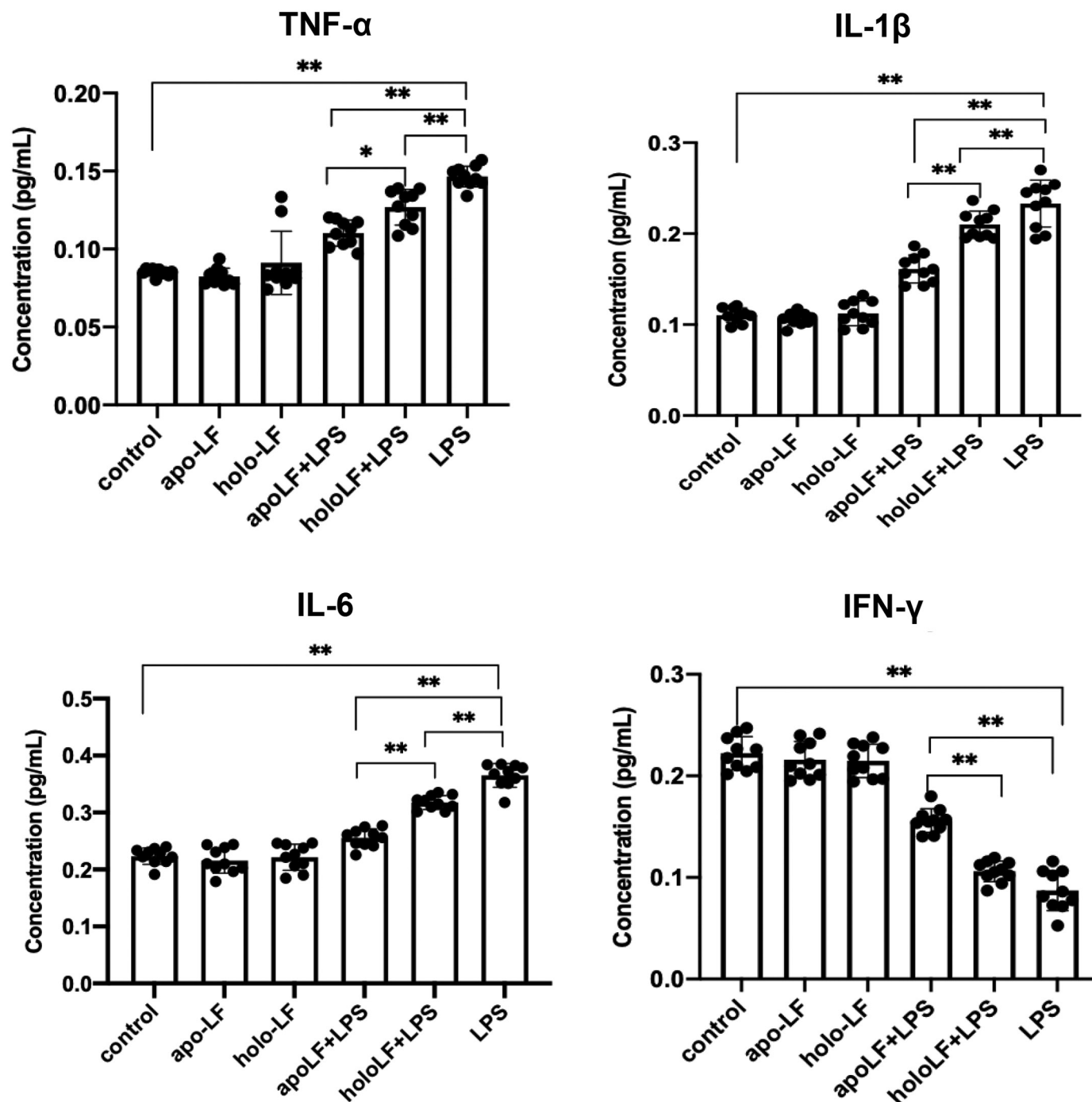


**Figure 2.** Expressions of inflammatory factors in colon tissue of young mice detected by ELISA methods. (A) The level of TNF- $\alpha$  (pg/mL) in colon tissue, (B) level of IL-1 $\beta$  (pg/mL) in colon tissue, (C) level of IL-6 (pg/mL) in colon tissue, and (D) level of INF- $\gamma$  (pg/mL) in colon tissue. The data are shown as mean  $\pm$  SD. Differences between groups were analyzed using Student's *t*-test. \**P* < 0.05, \*\**P* < 0.01, compared with the control, n = 8. apo-LF = iron-deficient lactoferrin; holo-LF = iron-saturated lactoferrin.

In the apo-LF+LPS group, the brown granules were partially reduced and the inflammatory injury was reduced, thus proving the regulatory role of apo-LF in protecting colon tissue from LPS stimulation (Figure 3B).

#### ***Apo-LF Suppression of Apo-LPS-Induced Enteritis Via the Regulation of the PPAR- $\gamma$ /PFKFB3/NF- $\kappa$ B Pathway***

In the intestinal epithelial cell model in vitro, 3 doses of LF and 3 doses of LF+LPS reaction (1, 5,

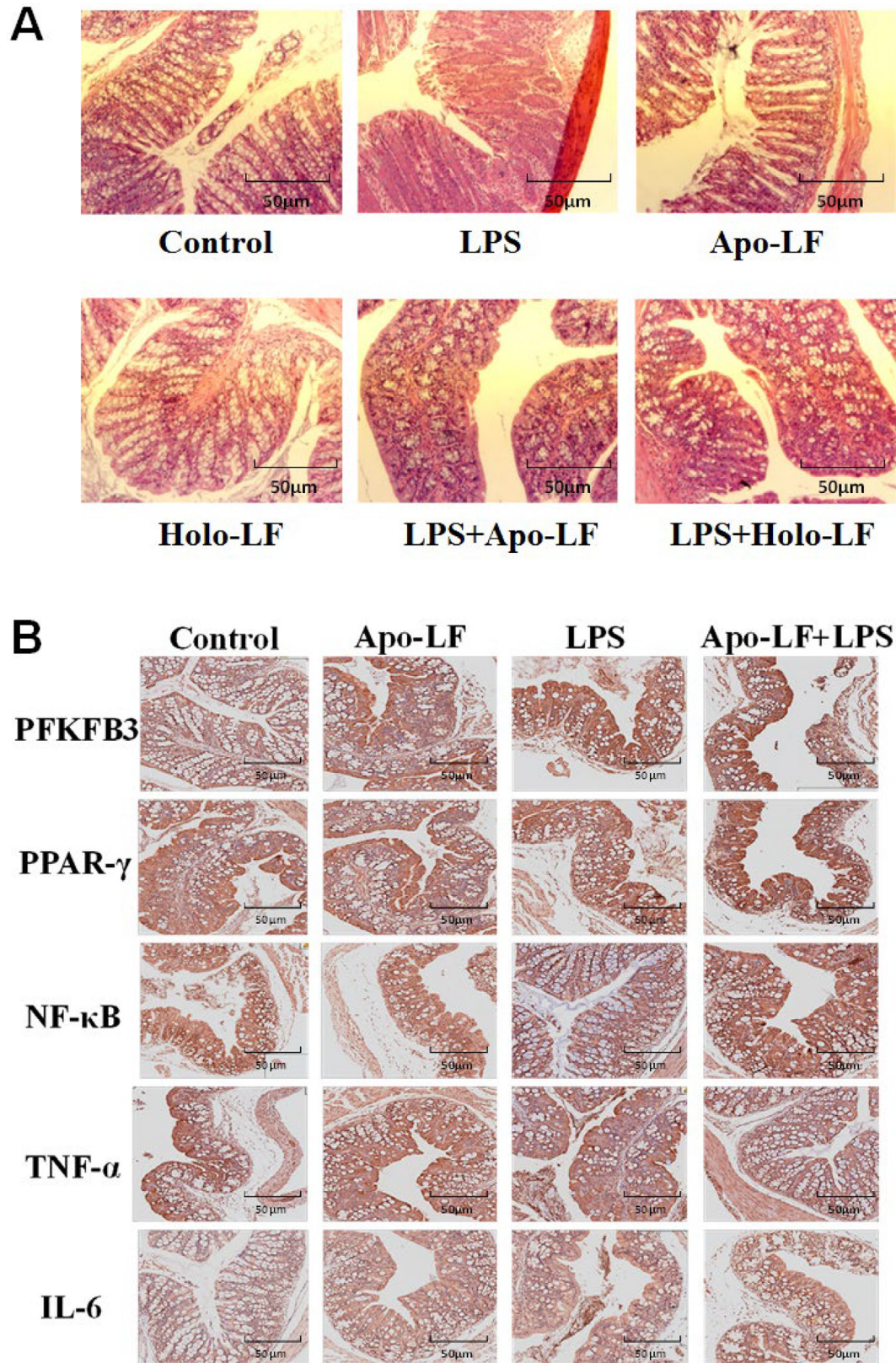


**Figure 3.** Pathological conditions of colon tissue and intestine tissue of young mice, stained by hematoxylin and eosin (HE) or 3,3'-diaminobenzidine (DAB). (A) The HE-stained sections of colon tissue in young mice, and (B) DAB staining results of mice colon tissue. The figures in each group were randomly captured under a 200× microscope, n = 3. apo-LF = iron-deficient lactoferrin; holo-LF = iron-saturated lactoferrin.



and 10 g/L) were given at a single time. After 48 h, the intestinal epithelial cells were collected, and the related proteins and genes were detected by WB and q-PCR. The results showed that of the 3 dose levels (1, 5, and 10 g/L) in PPAR- $\gamma$ , PFKFB3, NF- $\kappa$ B, TNF- $\alpha$ , and IL-1 $\beta$ , the dose of 10 g/L was the most appropriate. Therefore, in a further cell model, 10 g/L BW was selected as the appropriate dose of LF. Compared with the control, the mRNA and protein expression levels of PPAR- $\gamma$ , PFKFB3, NF- $\kappa$ B, TNF- $\alpha$ , and IL-1 $\beta$  proteins in apo-LF group showed no significant differences (Figure 4). The mRNA and levels of PPAR- $\gamma$  and PFKFB3 proteins were significantly decreased in the LPS group, whereas NF- $\kappa$ B, TNF- $\alpha$ , and IL-1 $\beta$  levels were significantly increased when compared with the control group ( $P < 0.01$ ; Figure 4A, C). In the LPS+LF treatment group, mRNA and PPAR- $\gamma$  and PFKFB3 protein levels significantly decreased, whereas the level of NF- $\kappa$ B significantly increased, and the levels of TNF- $\alpha$  and IL-1 $\beta$  were significantly downregulated ( $P < 0.01$ ; Figure 4A, C). These results further proved that apo-LF protects against LPS-induced intestinal inflammation injury by regulating PPAR- $\gamma$ , PFKFB3, and NF- $\kappa$ B pathways.

## DISCUSSION

Our experimental results show that both apo-LF and holo-LF can improve the intestinal inflammation of young mice induced by LPS, but the effect of apo-LF is stronger than holo-LF. This is consistent with the previously reported results of LF with different iron saturation (apo-LF and holo-LF stimulated promotion of mouse crypt cells but through different cellular signaling pathways). The experimental results show that apo-LF has a more obvious effect on stimulating the proliferation of crypt cells. The different effects of apo-LF and holo-LF may be due to the different molecular conformations caused by their different iron saturation, and the different physicochemical properties of LF that may affect the 2 iron saturations. In this study, in our in vitro model of young mice, holo-LF comes from purchase. The literature reports that its saturation is about 95%. The apo-LF was prepared according to the patent and its saturation was 4.1% (Sui et al., 2010; Bokkhim et al., 2013; Voswinkel et al., 2016). We mainly studied the improvement of 2 kinds of iron saturation on intestinal inflammation in young mice, according to the intestinal histopathological score of young mice. The most suitable type of LF was apo-LF. In the in vitro model, we stimulated primary intestinal epithelial cells of young mice with LPS and intervened with apo-LF. The DAB staining and WB results showed that apo-LF could effectively improve the inflammatory response of intestinal epithelial cells of young mice.

The LPS-induced colitis mouse model is mature and widely accepted, as its clinical manifestations and pathological changes are similar to those of human ulcerative colitis (Lönnerdal and Iyer, 1995). In in vitro and in vivo acute lung inflammation models, the concentrations of LPS were 1 mg/L in pulmonary cells and 10 mg/kg BW in mice, respectively (Li et al., 2021b). Thus, in the present study, primary intestinal epithelial cells were treated with LPS (1 mg/L), and C57BL/6J male mice were intraperitoneally injected with LPS solution (10 mg/kg BW) for 10 d to construct in vitro and in vivo intestinal inflammation damage models. Furthermore, the concentrations of LF in in vitro and in vivo acute lung inflammation models were 10 g/L and 100 mg/kg BW, respectively; therefore, we also used these 2 concentrations in this study (Li et al., 2021c). The mice in the LPS group developed typical features of ulcerative colitis, such as diarrhea, occult hematochezia, and gross hematochezia, among other symptoms. Colon tissues were found to be damaged in mucosa and glands. Under the light microscope, HE stains revealed a large number of inflammatory cell infiltrations and DAB staining revealed a large number of positive areas, confirming the successful construction of the animal model. Although the typical symptoms of colitis were also observed in the apo-LF+LPS mice, their symptoms of diarrhea, occult hematochezia, and gross hematochezia were significantly relieved in comparison to those of the LPS group. Moreover, their DAI and histopathological scores were significantly lower than those in the LPS group, and the pathological symptoms of intestinal mucosal inflammation and colon shortening were also significantly improved. The holo-LF+LPS mice were given intragastric administration and no difference was found between that group and the LPS group of mice. These results showed that, although LF could not prevent the occurrence of colitis, apo-LF had a significant colitis-alleviating effect, whereas holo-LF had no significant effect. Iron saturation was, thus, shown to have an effect on the alleviating effect of LF on ulcerative colitis. Therefore, in the animal experimental model in vitro, we selected apo-LF as the LF with the optimal iron saturation through intestinal tissue score, HE staining, and intestinal LPS concentration, so as to further verify the role of apo-LF in cells.

Intestinal immunity plays a significant role in the pathogenesis of ulcerative colitis (Dong et al., 2020), and proinflammatory cytokines TNF- $\alpha$ , IL-1 $\beta$ , IL-6, and INF- $\gamma$  are important mediators of immune response (Dinarello, 2011; Hermanns et al., 2016; Lazaridis et al., 2017; Nikolaus et al., 2018). In LPS-induced ulcerative colitis, a large number of inflammatory infiltrating cells secrete high levels of proinflammatory cytokines.

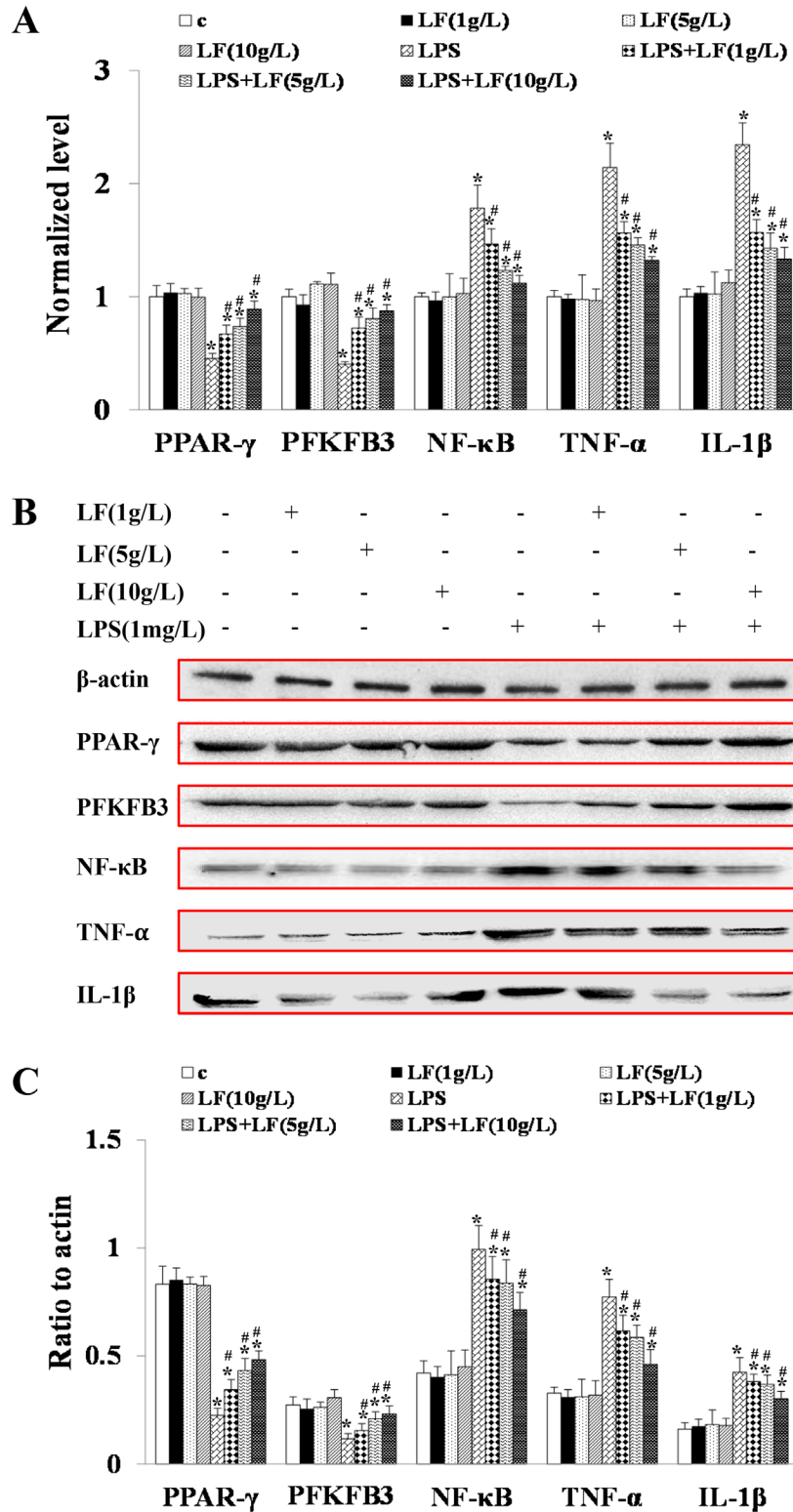


**Figure 4.** Expression levels of PPAR- $\gamma$ , PFKFB3, NF- $\kappa$ B, TNF- $\alpha$ , and IL-1 $\beta$  in colon tissues of young mice: (A) mRNA level of PPAR- $\gamma$ , PFKFB3, NF- $\kappa$ B, TNF- $\alpha$ , and IL-1 $\beta$  detected by reverse-transcription PCR; (B) protein bands of PPAR- $\gamma$ , PFKFB3, NF- $\kappa$ B, TNF- $\alpha$ , and IL-1 $\beta$  captured by a chemiluminescence apparatus; and (C) protein levels of PPAR- $\gamma$ , PFKFB3, NF- $\kappa$ B, TNF- $\alpha$ , and IL-1 $\beta$  detected by western blot. c = control; LF = lactoferrin. The data were analyzed by Image J software (Image J1.53a; National Institutes of Health) and are shown as mean  $\pm$  SD. Differences between groups were analyzed using Student's *t*-test. \**P* < 0.05 compared with the control, #*P* < 0.05 compared with the LPS group, n = 3.

Proinflammatory factors such as TNF- $\alpha$  and IL-1 $\beta$  induce inflammation by aggregating multinucleated cells in colon tissue, which is the direct pathogenesis of colitis (Cai et al., 2018). It was previously found that the inhibition of TNF- $\alpha$  and IL-6 expression is one of the antiinflammatory effects of LF in mice with LPS-induced ulcerative colitis (Kruzel et al., 2002). In this study, the expression levels of TNF- $\alpha$ , IL-1 $\beta$  and IL-1 $\beta$  in the colon tissues of the LPS group of mice were significantly decreased by the intragastric administration of apo-LF, whereas the expression levels of INF- $\gamma$  were significantly increased. No significant differences were observed between the holo-LF and LPS groups, which suggests that the differences between apo-LF and holo-LF in the mitigation of colitis may be due to the different effects of apo-LF on the expression of inflammatory factors. Other studies (Mu and Pang, 2011) reported that LF can bind to LF receptors on intestinal mucosa to regulate the intestinal immune response. The degree to which LF binds with intestinal LF receptors differs depending on its iron saturation and consequent structure, thus triggering different degrees of intestinal immune response, which may be one of the reasons for the differences in the colitis-alleviating effects of apo-LF and holo-LF.

A glycolipid occurring on the walls of most gram-negative bacteria, LPS is a potential and important source of inflammation. The interaction of LPS with a series of protein molecules leads eventually to the release of a variety of inflammatory cytokines and effector molecules, thereby promoting the adhesion of inflammatory cells (Holst et al., 1996; Rice et al., 2003). Previous studies (Puddu et al., 2010) have shown that the N-terminal positively charged region of LF can bind with negatively charged LPS, thereby blocking the activation of proinflammatory factor expression pathways and reducing the risk of inflammation. In this study, apo-LF was found to significantly reduce the concentration of LPS in the intestinal tracts of mice in the apo-LF group by inhibiting the growth of gram-negative bacteria to reduce the source of LPS and by combining with LPS, thus indicating its role in alleviating the inflammatory response. Furthermore, research (Bellamy et al., 1992) has confirmed that the binding of LF and LPS occurs in a different region from the iron binding site. The *in vitro* test of this study also proved that, although no significant difference was observed in the binding abilities of apo-LF and holo-LF to LPS, there was also no significant difference in the LPS concentrations in the intestines of the holo-LF and control groups. This may be due to the weak inhibition ability of holo-LF against gram-negative bacteria and the absence of a significant reduction in the source of LPS.

In the past decade, it has been found that programmed cell necrosis requires PPAR- $\gamma$ , PFKFB3, and NF- $\kappa$ B proteins, which can be activated by interferon, death receptors, and intracellular RNA and DNA sensors, among others. PPAR $\gamma$  is induced before the transcriptional activation of many adipocyte genes and plays an important role in cell differentiation (Houseknecht et al., 2002). Furthermore, its antiproliferation, preset apoptosis, and differentiation functions (Bishop-Bailey et al., 2003) indicate the comprehensive anticancer activity of PPAR $\gamma$ . Ulcerative colitis is closely related to the occurrence of colon cancer, and PPAR- $\gamma$  agonists can inhibit the activation of macrophages and the generation of inflammatory cytokines, and inhibit the progression of inflammation and tumorigenesis (Ricote et al., 1998). In addition, PFKFB3 was found to be highly expressed in proliferating tissues, transformed cells, solid tumors, and leukemia cells. The expression of PFKFB3 can be upregulated in response to mitotic, inflammatory, and hypoxic stimuli, as well as during the DNA synthesis phase of the cell cycle (Atsumi et al., 2002). However, the role of PFKFB3 in intestinal inflammation damage, which may also be one of the pathways regulating inflammatory damage, has not been fully investigated. The NF- $\kappa$ B signaling pathway is one of the important pathways for the regulation of inflammatory responses. As a key factor in this pathway, NF- $\kappa$ B subunit NF- $\kappa$ Bp65 is highly expressed in the colonic mucosa of patients with ulcerative colitis, thereby damaging the physiological barrier of mucosa, leading to increased colonic permeability and promoting the progression of ulcerative colitis (Williams et al., 2013). NF- $\kappa$ B signaling in immune cells drives the expression of proinflammatory cytokines such as TNF- $\alpha$  or IL-1 $\beta$ , which then activate NF- $\kappa$ B in intestinal epithelial cells, thereby promoting cell survival (Williams et al., 2013). In support of this, TNF- $\alpha$  administration of NF- $\kappa$ B1 mice has been reported to demonstrate increased intestinal epithelial apoptosis (Williams et al., 2013).

In this study, the optimal type of LF was selected as apo-LF in the animal models to guide the *in vitro* cell experiments, and the protective effect of apo-LF on intestinal epithelial cells was further verified via primary intestinal epithelial cells. By immune imprinting, we found that the expressions of PPAR- $\gamma$ , PFKFB3, and NF- $\kappa$ B genes and proteins in the intestinal epithelial cells of the mice were altered, which could inhibit the inflammation of colon mucosa and repair mucosal injury. The results showed that the protein expression of NF- $\kappa$ B was high in the LPS group, whereas the protein expressions of PPAR- $\gamma$  and PFKFB3 were low. After apo-LF treatment, the protein expression of NF- $\kappa$ B was

significantly downregulated, whereas those of PPAR- $\gamma$  and PFKFB3 were upregulated. These results suggest that apo-LF may reduce the release of inflammatory factors by inhibiting the NF- $\kappa$ B signaling pathway and activating PPAR- $\gamma$  and PFKFB3 signaling pathways, thereby reducing intestinal mucosal inflammation and repairing intestinal mucosal injury.

In conclusion, the optimal type of LF protein was selected as apo-LF in the mouse animal model, and we found that apo-LF could inhibit colon mucosal inflammation and repair mucosal injury by regulating the expressions of PPAR- $\gamma$ , PFKFB3 and NF- $\kappa$ B genes and proteins. Finally, the mechanism by which LF protects intestinal inflammation injury in infants and young children was analyzed.

### ACKNOWLEDGMENTS




We are grateful for support from 2 key laboratories: the Key Laboratory of Quality and Safety Control for Milk and Dairy Products, and the Laboratory of Quality and Safety Risk Assessment for Dairy Products, Ministry of Agriculture and Rural Affairs, China. We are grateful for support from the Scientific Research Project for Major Achievements of the Agricultural Science and Technology Innovation Program (ASTIP; Beijing, China; no. CAAS-ZDXT2019004), the Ministry of Modern Agro-Industry Technology Research System of China (CARS-36), and the Agricultural Science and Technology Innovation Program (ASTIP-IAS12). The authors have not stated any conflicts of interest.

### REFERENCES

- Atsumi, T., J. Chesney, C. Metz, L. Leng, S. Donnelly, Z. Makita, R. Mitchell, and R. Bucala. 2002. High expression of inducible 6-phosphofructo-2-kinase/fructose-2,6-bisphosphatase (iPFK-2; PFKFB3) in human cancers. *Cancer Res.* 62:5881–5887.
- Baker, H. M., and E. N. Baker. 2004. Lactoferrin and iron: Structural and dynamic aspects of binding and release. *Biometals* 17:209–216. <https://doi.org/10.1023/B:BIOM.0000027694.40260.70>.
- Battersby, C., N. Longford, S. Mandalia, K. Costeloe, and N. Modi. 2017. Incidence and enteral feed antecedents of severe neonatal necrotising enterocolitis across neonatal networks in England, 2012–13: A whole-population surveillance study. *Lancet Gastroenterol. Hepatol.* 2:43–51. [https://doi.org/10.1016/S2468-1253\(16\)30117-0](https://doi.org/10.1016/S2468-1253(16)30117-0).
- Battersby, C., T. Santhalingam, K. Costeloe, and N. Modi. 2018. Incidence of neonatal necrotising enterocolitis in high-income countries: A systematic review. *Arch. Dis. Child Fetal Neonatal Ed.* 103:F182–F189. <https://doi.org/10.1136/archdischild-2017-313880>.
- Bellamy, W., M. Takase, K. Yamauchi, H. Wakabayashi, K. Kawase, and M. Tomita. 1992. Identification of the bactericidal domain of lactoferrin. *Biochim. Biophys. Acta* 1121:130–136. [https://doi.org/10.1016/0167-4838\(92\)90346-F](https://doi.org/10.1016/0167-4838(92)90346-F).
- Bishop-Bailey, D., and T. D. Warner. 2003. PPAR gamma ligands induce prostaglandin production in vascular smooth muscle cells: Indomethacin acts as a peroxisome proliferator-activated receptor-gamma antagonist. *FASEB J.* 17:1925–1927. <https://doi.org/10.1096/fj.02-1075fje>.
- Black, R. E., S. Cousens, H. L. Johnson, J. E. Lawn, I. Rudan, and D. G. Bassani. 2010. Global, regional, and national causes of child mortality in 2008: A systematic analysis. *Lancet* 375:1969–1987. [https://doi.org/10.1016/S0140-6736\(10\)60549-1](https://doi.org/10.1016/S0140-6736(10)60549-1).
- Bokkhim, H., N. Bansal, L. Gröndahl, and B. Bhandari. 2013. Physico-chemical properties of different forms of bovine lactoferrin. *Food Chem.* 141:3007–3013. <https://doi.org/10.1016/j.foodchem.2013.05.139>.
- Cai, Z., P. Xu, Z. Wu, and D. Pan. 2018. Anti-inflammatory activity of surface layer protein SLPA of *Lactobacillus acidophilus* CICC 6074 in LPS-induced raw 264.7 cells and DSS-induced mice colitis. *J. Funct. Foods* 51:16–27. <https://doi.org/10.1016/j.jff.2018.10.008>.
- Dinarello, C. A. 2011. Interleukin-1 in the pathogenesis and treatment of inflammatory diseases. *Blood* 117:3720–3732. <https://doi.org/10.1182/blood-2010-07-273417>.
- Dong, N., X. Li, C. Xue, L. Zhang, C. Wang, X. Xu, and A. Shan. 2020. Astragalus polysaccharides alleviates LPS-induced inflammation via the NF- $\kappa$ B/MAPK signaling pathway. *J. Cell. Physiol.* 235:5525–5540. <https://doi.org/10.1002/jcp.29452>.
- Fitzsimons, D. W. 2013. World Health Organization. *Acta Med. Port.* 26:186–187.
- Grisham, M. B., and T. Yamada. 1992. Neutrophils, nitrogen oxides, and inflammatory bowel disease. *Ann. N. Y. Acad. Sci.* 664(1 Neuro-immuno-):103–115. <https://doi.org/10.1111/j.1749-6632.1992.tb39753.x>.
- Grossmann, J. G., M. Neu, E. Pantos, F. J. Schwab, R. W. Evans, E. Townes-Andrews, P. F. Lindley, H. Appel, W. G. Thies, and S. S. Hasnain. 1992. X-ray solution scattering reveals conformational changes upon iron uptake in lactoferrin, serum and ovotransferrins. *J. Mol. Biol.* 225:811–819. [https://doi.org/10.1016/0022-2836\(92\)90402-6](https://doi.org/10.1016/0022-2836(92)90402-6).
- Hering, N. A., J. Luettig, S. M. Krug, S. Wiegand, G. Gross, E. A. van Tol, J. D. Schulzke, and R. Rosenthal. 2017. Lactoferrin protects against intestinal inflammation and bacteria-induced barrier dysfunction in vitro. *Ann. N. Y. Acad. Sci.* 1405:177–188. <https://doi.org/10.1111/nyas.13405>.
- Hermanns, H. M., J. Wohlfahrt, C. Mais, S. Hergovits, D. Jahn, and A. Geier. 2016. A Geier endocytosis of pro-inflammatory cytokine receptors and its relevance for signal transduction. *Biol. Chem.* 397:695–708. <https://doi.org/10.1515/hsz-2015-0277>.
- Holst, O., A. J. Ulmer, H. Brade, H.-D. Flad, and E. Th. Rietschel. 1996. Biochemistry and cell biology of bacterial endotoxins. *FEMS Immunol. Med. Microbiol.* 16:83–104. <https://doi.org/10.1111/j.1574-695X.1996.tb00126.x>.
- Houseknecht, K. L., B. M. Cole, and P. J. Steele. 2002. Peroxisome proliferator-activated receptor gamma (PPAR $\gamma$ ) and its ligands: A review. *Domest. Anim. Endocrinol.* 22:1–23. [https://doi.org/10.1016/S0739-7240\(01\)00117-5](https://doi.org/10.1016/S0739-7240(01)00117-5).
- Jiang, R. L., and B. Lönnerdal. 2012. Apo- and holo-lactoferrin stimulate proliferation of mouse crypt cells but through different cellular signaling pathways. *Int. J. Biochem. Cell Biol.* 44:91–100. <https://doi.org/10.1016/j.biocel.2011.10.002>.
- Kanwar, J., Y. Patel, K. Roy, R. Kanwar, R. Rajkhowa, and X. Wang. 2015. Biodegradable Eri silk nanoparticles as a delivery vehicle for bovine lactoferrin against MDA-MB-231 and MCF-7 breast cancer cells. *Int. J. Nanomedicine* 11:25–44. <https://doi.org/10.2147/IJN.S91810>.
- Kruzal, M. L., Y. Harari, D. Mailman, J. K. Actor, and M. Zimecki. 2002. Differential effects of prophylactic, concurrent and therapeutic lactoferrin treatment on LPS-induced inflammatory responses in mice. *Clin. Exp. Immunol.* 130:25–31. <https://doi.org/10.1046/j.1365-2249.2002.01956.x>.
- Lazaridis, L. D., A. Pistiki, E. J. Giamarellos-Bourboulis, M. Georgitsi, G. Damoraki, D. Polymeros, G. D. Dimitriadis, and K. Triantafyllou. 2017. Activation of NLRP3 inflammasome in inflammatory bowel disease: Differences between Crohn's disease and ulcerative colitis. *Dig. Dis. Sci.* 62:2348–2356. <https://doi.org/10.1007/s10620-017-4609-8>.

- Li, H. Y., P. Li, H. G. Yang, Y. Z. Wang, G. X. Huang, J. Q. Wang, and N. Zheng. 2019. Investigation and comparison of the anti-tumor activities of lactoferrin,  $\alpha$ -lactalbumin, and  $\beta$ -lactoglobulin in a549, ht29, hepg2, and mda231-lm2 tumor models. *J. Dairy Sci.* 102:9586–9597. <https://doi.org/10.3168/jds.2019-16429>.
- Li, H. Y., H. G. Yang, H. M. Wu, Q. Q. Yao, Z. Y. Zhang, Q. S. Meng, L. L. Fan, J. Q. Wang, and N. Zheng. 2021a. Inhibitory effects of lactoferrin on pulmonary inflammatory processes induced by lipopolysaccharide by modulating the TLR4-related pathway. *J. Dairy Sci.* 104:7383–7392. <https://doi.org/10.3168/jds.2020-19232>.
- Li, M., C. Wang, H. G. Wu, S. Y. Lv, Q. Qi, F. Li, H. R. Liu, X. M. Wang, and L. Y. Wu. 2021b. Effect of moxibustion on LPS/TLR4 signaling pathway in colonic tissue of rats with ulcerative colitis. *World Traditional Chin. Med.* 2021:1–21.
- Lönnerdal, B., and S. Iyer. 1995. Lactoferrin-molecular-structure and biological function. *Annu. Rev. Nutr.* 15:93–110. <https://doi.org/10.1146/annurev.nu.15.070195.000521>.
- Lu, R. R., S. Y. Xu, R. J. Yang, and Z. Sun. 2008. Antimicrobial activity of lactoferrin and its mechanism involved. *Shipin Xue* 29:238–243. <https://doi.org/10.16429/j.1009-7848.2014.10.013>.
- Luo, S. B., C. Y. Wang, L. L. Yang, Y. Cheng, Z. Y. Yun, and J. W. Yang. 2020. A method for preparing lactoferrin with required iron saturation. Inner Mongolia Yili Industrial Group Co. Ltd., assignee. Application No. 201810713582.
- Mu, L., and G. C. Pang. 2011. Research progress of mammalian intestinal lactoferrin receptor and its function. *Food Sci.* 32:312–316.
- Murano, M., K. Maemura, I. Hirata, K. Toshina, T. Nishikawa, N. Hamamoto, S. Sasaki, O. Saitoh, and K. Katsu. 2001. Therapeutic effect of intracolonic administered nuclear factor kappa B(p65) antisense oligonucleotide on mouse dextran sulphate sodium(DSS)-induced colitis. *Clin. Exp. Immunol.* 120:51–58. <https://doi.org/10.1046/j.1365-2249.2000.01183.x>.
- Nabulsi, M., N. Yazbeck, and F. Charafeddine. 2015. Lactose-free milk for infants with acute gastroenteritis in a developing country: Study protocol for a randomized controlled trial. *Trials* 16:46. <https://doi.org/10.1186/s13063-015-0565-9>.
- Niaz, B., F. Saeed, A. Ahmed, M. Imran, A. A. Maan, M. K. I. Khan, T. Tufail, F. M. Anjum, S. Hussain, and H. A. R. Suleria. 2019. Lactoferrin (LF): A natural antimicrobial protein. *Int. J. Food Prop.* 22:1626–1641. <https://doi.org/10.1080/10942912.2019.1666137>.
- Nikolaus, S., G. H. Waetzig, S. Butzin, M. Ziolkiewicz, N. Al-Massad, F. Thieme, U. Lövgren, B. B. Rasmussen, T. M. Reinheimer, D. Seeger, P. Rosenstiel, S. Szymczak, and S. Schreiber. 2018. Evaluation of interleukin-6 and its soluble receptor components sIL-6R and sgp130 as markers of inflammation in inflammatory bowel diseases. *Int. J. Colorectal Dis.* 33:927–936. <https://doi.org/10.1007/s00384-018-3069-8>.
- NRC. 2001. Nutrient Requirements of Dairy Cattle. National Academies Press.
- Peterson, L. W., and D. Artis. 2014. Intestinal epithelial cells: Regulators of barrier function and immune homeostasis. *Nat. Rev. Immunol.* 14:141–153. <https://doi.org/10.1038/nri3608>.
- Puddu, P., D. Latorre, P. Valenti, and S. Gessani. 2010. Immunoregulatory role of lactoferrin-lipopolysaccharide interactions. *Biomaterials* 23:387–397. <https://doi.org/10.1007/s10534-010-9307-3>.
- Rice, J. B., L. L. Stoll, W.-G. Li, G. M. Denning, J. Weydert, E. Charipar, W. E. Richenbacher, F. J. Miller Jr., and N. L. Weintraub. 2003. Low-level endotoxin induces potent inflammatory activation of human blood vessels: Inhibition by statins. *Arterioscler. Thromb. Vasc. Biol.* 23:1576–1582. <https://doi.org/10.1161/01.ATV.0000081741.38087.F9>.
- Richter, K. K., M. K. Fagerhol, J. C. Carr, J. M. Winkler, C. C. Sung, and M. Hauer-Jensen. 1997. Association of granulocyte transmigration with structural and cellular parameters of injury in experimental radiation enteropathy. *Radiat. Oncol. Investig.* 5:275–282. [https://doi.org/10.1002/\(SICI\)1520-6823\(1997\)5:6<275::AID-ROI3>3.0.CO;2-V](https://doi.org/10.1002/(SICI)1520-6823(1997)5:6<275::AID-ROI3>3.0.CO;2-V).
- Ricote, M., A. C. Li, T. M. Willson, C. J. Kelly, and C. K. Glass. 1998. The peroxisome proliferators-activated receptor is a negative regulator of macrophage activation. *Nature* 391:79–82. <https://doi.org/10.1038/34178>.
- Scalaferrì, F., and C. Fiocchi. 2007. Inflammatory bowel disease: Progress and current concept of etiopathogenesis. *J. Dig. Dis.* 8:171–178. <https://doi.org/10.1111/j.1751-2980.2007.00310.x>.
- Sui, Q., H. Roginski, R. P. Williams, C. Versteeg, and J. Wan. 2010. Effect of pulsed electric field and thermal treatment on the physicochemical properties of lactoferrin with different iron saturation levels. *Int. Dairy J.* 20:707–714. <https://doi.org/10.1016/j.idairyj.2010.03.013>.
- Villaseca, J. M., U. Hernández, T. R. Sainz-Espues, C. Rosario, and C. Eslava. 2005. Enteroaggregative *Escherichia coli* an emergent pathogen with different virulence properties. *Rev. Latinoam. Microbiol.* 47:140–159.
- Voswinkel, L., T. Vogel, and U. Kulozik. 2016. Impact of the iron saturation of bovine lactoferrin on adsorption to a strong cation exchanger membrane. *Int. Dairy J.* 56:134–140. <https://doi.org/10.1016/j.idairyj.2016.01.008>.
- Williams, J. M., C. A. Duckworth, A. J. Watson, M. R. Frey, J. C. Miguel, M. D. Burkitt, R. Sutton, K. R. Hughes, L. J. Hall, J. H. Caamano, B. J. Campbell, and D. M. Pritchard. 2013. A mouse model of pathological small intestinal epithelial cell apoptosis and shedding induced by systemic administration of lipopolysaccharide. *Dis. Model. Mech.* 6:1388–1399. <https://doi.org/10.1242/dmm.013284>.
- Xia, D. Y., L. Yang, Y. W. Zhu, and W. C. Wang. 2021. Analysis of lipopolysaccharide content in chyme microbiota of waterfowl cecum. *Microbiome Protocols eBook Biol.* 101:e2003747. <https://doi.org/10.21769/BioProtoc.2003747>.
- Yu, Y., L. Lu, J. Sun, E. O. Petrof, and E. C. Claud. 2016. Preterm infant gut microbiota affects intestinal epithelial development in a humanized microbiome gnotobiotic mouse model. *Am. J. Physiol. Gastrointest. Liver Physiol.* 311:G521. <https://doi.org/10.1152/ajpgi.00022.2016>.
- Zhao, W., Y. Wang, S. Liu, J. Huang, Z. Zhai, C. He, J. Ding, J. Wang, H. Wang, W. Fan, J. Zhao, and H. Meng. 2015. The dynamic distribution of porcine microbiota across different ages and gastrointestinal tract segments. *PLoS One* 10:e0117441. <https://doi.org/10.1371/journal.pone.0117441>.
- Zhang, H., M. Shao, H. Huang, S. Wang, L. Ma, H. Wang, L. Hu, K. Wei, and R. Zhu. 2018. The dynamic distribution of small-tail Han sheep microbiota across different intestinal segments. *Front. Microbiol.* 9:32. <https://doi.org/10.3389/fmicb.2018.00032>.
- Zhou, Y., G. Shan, E. Sodergren, G. Weinstock, W. A. Walker, and K. E. Gregory. 2015. Longitudinal analysis of the premature infant intestinal microbiome prior to necrotizing enterocolitis: A case-control study. *PLoS One* 10:e0118632. <https://doi.org/10.1371/journal.pone.0118632>.

## ORCID

- H. M. Wu  <https://orcid.org/0000-0003-0648-4328>  
 J. Q. Wang  <https://orcid.org/0000-0001-8841-0124>  
 N. Zheng  <https://orcid.org/0000-0002-5365-9680>